Calculation of Free Baryon Spectral densities at finite Temperature

Chrisanthi Praki

Swansea University

July 2015

with Gert Aarts, Chris Allton, Simon Hands, Benjamin Jaeger (Swansea University), Jon-Ivar Skullerud (National University of Ireland, Maynooth)

Motivations

- The presence of a thermal medium (hadronic plasma, quark-gluon plasma) may effect the properties of hadrons:
  - thermal mass shift
  - thermal broadening
  - melting/dissolution ...

Motivations

- The presence of a thermal medium (hadronic plasma, quark-gluon plasma) may effect the properties of hadrons:
  - thermal mass shift
  - thermal broadening
  - melting/dissolution ...
- In-medium effects have been intensely studied for mesons
  - dileptons
  - chiral symmetry
  - quarkonium ...

Motivations

- The presence of a thermal medium (hadronic plasma, quark-gluon plasma) may effect the properties of hadrons:
  - thermal mass shift
  - thermal broadening
  - melting/dissolution ...
- In-medium effects have been intensely studied for mesons
  - dileptons
  - chiral symmetry
  - quarkonium ...
- There have been very few similar studies for baryons
  - DeTar & Kogut (1987)
  - Pushkina *et al.* (2005)
  - Datta, Gupta, Padmanath, Maiti & Mathur (2013)

Motivations

- The presence of a thermal medium (hadronic plasma, quark-gluon plasma) may effect the properties of hadrons:
  - thermal mass shift
  - thermal broadening
  - melting/dissolution ...
- In-medium effects have been intensely studied for mesons
  - dileptons
  - chiral symmetry
  - quarkonium ...
- There have been very few similar studies for baryons
  - DeTar & Kogut (1987)
  - Pushkina *et al.* (2005)
  - Datta, Gupta, Padmanath, Maiti & Mathur (2013)
- See the next talk by Chris Allton with $N_f = 2 + 1$ simulations the first detailed study of nucleons at finite temperature on the lattice, also Phys. Rev. D **92**, 014503 (2015).

Introduction

In this talk:

- We study discretisation effects in the calculation of spectral densities of free nucleon-nucleon correlators at finite temperature by comparing continuum and lattice spectral functions.

Introduction

In this talk:

- We study discretisation effects in the calculation of spectral densities of free nucleon-nucleon correlators at finite temperature by comparing continuum and lattice spectral functions.
- In particular, we will analyse the lattice artifacts at higher energies.

Free Hadron Propagator

The free hadron propagator may be calculated by considering a hadron composed of three non-interacting quarks produced at a point (0,t) and propagating to the point $(\mathbf{x}, t)$ where it annihilates.

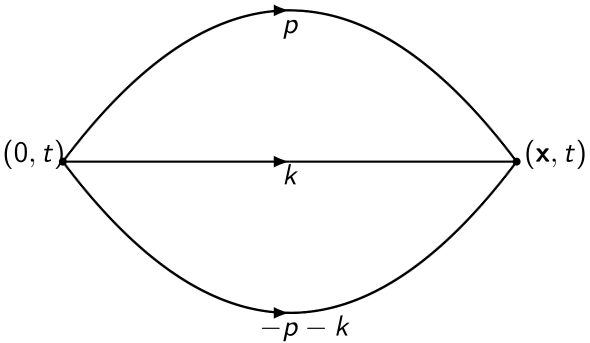

Correlation Function

- In order to calculate the two point correlation function for the proton, we introduce the nucleon creation and annihilation operators

$$O^{\alpha}(x) = \epsilon_{abc}[d_a^T(x)C^{-1}\gamma_5 u_b(x)]u_c^{\alpha}(x) \quad (1)$$

$$\bar{O}^{\alpha'}(x) = \epsilon_{a'b'c'}\bar{u}_{a'}^{\alpha'}(x)[\bar{u}_{b'}(x)\gamma_5 C\bar{d}_{c'}^T(x)]. \quad (2)$$

The charge conjugation matrix is defined as $C = i\gamma_2\gamma_4$.

Correlation Function

- In order to calculate the two point correlation function for the proton, we introduce the nucleon creation and annihilation operators

$$O^{\alpha}(x) = \epsilon_{abc}[d_a^T(x)C^{-1}\gamma_5 u_b(x)]u_c^{\alpha}(x) \tag{1}$$

$$\bar{O}^{\alpha'}(x) = \epsilon_{a'b'c'}\bar{u}_{a'}^{\alpha'}(x)[\bar{u}_{b'}(x)\gamma_5 C\bar{d}_{c'}^T(x)]. \tag{2}$$

  The charge conjugation matrix is defined as $C = i\gamma_2\gamma_4$.
- The following decomposition of the quark propagator is utilised

$$S = \langle\psi_a^{\alpha}(x)\bar{\psi}_b^{\beta}\rangle = S_4(x)\gamma_4 + S_i(x)\gamma_i + \mathrm{I}_4 S_m(x) \tag{3}$$

  where $\psi = u, d,\ i = 1, 2, 3.$

Correlation Function

- In order to calculate the two point correlation function for the proton, we introduce the nucleon creation and annihilation operators

$$O^{\alpha}(x) = \epsilon_{abc}[d_a^T(x)C^{-1}\gamma_5 u_b(x)]u_c^{\alpha}(x) \tag{1}$$

$$\bar{O}^{\alpha'}(x) = \epsilon_{a'b'c'}\bar{u}_{a'}^{\alpha'}(x)[\bar{u}_{b'}(x)\gamma_5 C\bar{d}_{c'}^T(x)]. \tag{2}$$

  The charge conjugation matrix is defined as $C = i\gamma_2\gamma_4$.
- The following decomposition of the quark propagator is utilised

$$S = \langle \psi_a^{\alpha}(x)\bar{\psi}_b^{\beta}\rangle = S_4(x)\gamma_4 + S_i(x)\gamma_i + \mathrm{I}_4 S_m(x) \tag{3}$$

  where $\psi = u, d,\ i = 1, 2, 3$.
- The two point correlation function may then be expressed as a combination of gamma matrices and B coefficients.

$$G^{\alpha\alpha'}(x) = \langle O^{\alpha}(x)\bar{O}^{\alpha'}(x)\rangle = B_4(x)\gamma_4 + B_i(x)\gamma_i + \mathrm{I}_4 B_m(x) \tag{4}$$

B Coefficients

$$G^{\alpha\alpha'}(x) = \langle O^{\alpha}(x)\bar{O}^{\alpha'}(x)\rangle = B_4(x)\gamma_4 + B_i(x)\gamma_i + \mathrm{I}_4 B_m(x) \quad (5)$$

- the B coefficients are given by

$$\begin{aligned} B_{\mu} &= 6S_{\mu}(5\sum_{\nu} S_{\nu}S_{\nu} + 7S_m S_m) \\ B_m &= 6S_m(7\sum_{\nu} S_{\nu}S_{\nu} + 5S_m S_m) \end{aligned} \quad (6)$$

where, for simplicity, we have used degenerate light quarks, $u = d = l$.

B Coefficients

$$G^{\alpha\alpha'}(x) = \langle O^{\alpha}(x)\bar{O}^{\alpha'}(x)\rangle = B_4(x)\gamma_4 + B_i(x)\gamma_i + \mathrm{I}_4 B_m(x) \qquad (5)$$

- the B coefficients are given by

$$\begin{aligned} B_\mu &= 6S_\mu(5\sum_\nu S_\nu S_\nu + 7S_m S_m) \\ B_m &= 6S_m(7\sum_\nu S_\nu S_\nu + 5S_m S_m) \end{aligned} \qquad (6)$$

  where, for simplicity, we have used degenerate light quarks, $u = d = l$.
- In order to determine the spectral functions for the proton, the B coefficients are re-expressed in terms of an integral over a kernel and the spectral function.

Spectral Functions

- For mesons, the spectral relations are given by $(\tilde{\tau} = \tau - 1/2T)$

$$G(\tau) = \int_{-\infty}^{\infty} \frac{d\omega}{2\pi} K(\tau,\omega)\rho(\omega), \qquad K(\tau,\omega) = \frac{\cosh(\tilde{\tau}\omega)}{\sinh(\omega/2T)} \tag{7}$$

Spectral Functions

- For mesons, the spectral relations are given by ($\tilde{\tau} = \tau - 1/2T$)

$$G(\tau) = \int_{-\infty}^{\infty} \frac{d\omega}{2\pi} K(\tau,\omega)\rho(\omega), \qquad K(\tau,\omega) = \frac{\cosh(\tilde{\tau}\omega)}{\sinh(\omega/2T)} \tag{7}$$

- For baryons the spectral relations are more complicated

$$\begin{aligned} B_4(\tau) &= \int_{-\infty}^{\infty} \frac{d\omega}{2\pi} K_e(\tau,\omega)\rho_4(\omega), \\ B_{i,m}(\tau) &= \int_{-\infty}^{\infty} \frac{d\omega}{2\pi} K_o(\tau,\omega)\rho_{i,m}(\omega), \end{aligned} \tag{8}$$

where the kernels are given by

$$\begin{aligned} K_e(\tau,\omega) &= \frac{\cosh(\tilde{\tau}\omega)}{\cosh(\omega/2T)} = [1 - n_F(\omega)]e^{-\omega\tau} + n_F(\omega)e^{\omega\tau}, \\ K_o(\tau,\omega) &= -\frac{\sinh(\tilde{\tau}\omega)}{\cosh(\omega/2T)} = [1 - n_F(\omega)]e^{-\omega\tau} - n_F(\omega)e^{\omega\tau} \end{aligned} \tag{9}$$

where $n_F(\omega) = 1/(e^{\omega/T} + 1)$ is the Fermi distribution.

Spectral Functions

- For mesons, the spectral relations are given by ($\tilde{\tau} = \tau - 1/2T$)

$$G(\tau) = \int_{-\infty}^{\infty} \frac{d\omega}{2\pi} K(\tau, \omega)\rho(\omega), \qquad K(\tau, \omega) = \frac{\cosh(\tilde{\tau}\omega)}{\sinh(\omega/2T)} \tag{7}$$

- For baryons the spectral relations are more complicated

$$\begin{aligned} B_4(\tau) &= \int_{-\infty}^{\infty} \frac{d\omega}{2\pi} K_e(\tau, \omega)\rho_4(\omega), \\ B_{i,m}(\tau) &= \int_{-\infty}^{\infty} \frac{d\omega}{2\pi} K_o(\tau, \omega)\rho_{i,m}(\omega), \end{aligned} \tag{8}$$

where the kernels are given by

$$\begin{aligned} K_e(\tau, \omega) &= \frac{\cosh(\tilde{\tau}\omega)}{\cosh(\omega/2T)} = [1 - n_F(\omega)]e^{-\omega\tau} + n_F(\omega)e^{\omega\tau}, \\ K_o(\tau, \omega) &= -\frac{\sinh(\tilde{\tau}\omega)}{\cosh(\omega/2T)} = [1 - n_F(\omega)]e^{-\omega\tau} - n_F(\omega)e^{\omega\tau} \end{aligned} \tag{9}$$

where $n_F(\omega) = 1/(e^{\omega/T} + 1)$ is the Fermi distribution.

- Note: $\lim_{T\to 0} K_{o,e}(\tau, \omega) = e^{-\omega\tau}$.

Parity

The parity projector is defined as $\mathrm{P}_{\pm} = \frac{1}{2}(\mathrm{I}_4 \pm \gamma_4)$.

$$\begin{aligned} G_{\pm}(\tau) &= \int d^3x \,\mathrm{tr}\, \mathrm{P}_{\pm} G(x) = \int d^3x \,\mathrm{tr}\, \langle \mathrm{P}_{\pm} O(x) \bar{O}(0) \rangle \\ &= 2(B_m(\tau) \pm B_4(\tau)) \end{aligned} \tag{10}$$

We can express $G_{\pm}$ in terms of the spectral functions with positive and negative parity.

$$G_{\pm}(\tau) = \int_{-\infty}^{\infty} \frac{d\omega}{2\pi} \left[\frac{e^{-\omega\tau}}{1+e^{-\omega/T}} \rho_{\pm}(\omega) - \frac{e^{-\omega(\tau-1/T)}}{1+e^{-\omega/T}} \rho_{\mp}(\omega) \right] \tag{11}$$

with $\rho_{\pm}(\omega) = 2\rho_m(\omega) \pm 2\rho_4(\omega)$.

Contributing Processes: Two-loop Calculation

There will be contributions to the spectral function from the decay of a proton into 3 quarks with momentum **p**, **k** and **r**, the reverse process and also all possible scattering processes. The different combinations can be determined by "cutting" the diagram for the proton propagator.

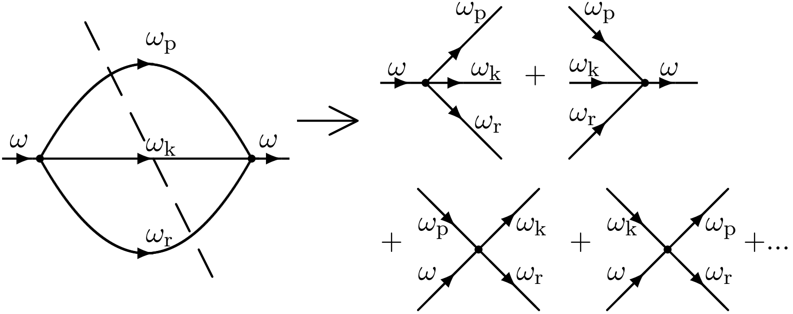

The processes which contribute to the spectral functions are therefore given by $\omega = \pm\omega_p \pm \omega_k \pm \omega_r$.

- The spectral densities may be written as

$$\rho_c(\omega) = 3 \int_{\mathbf{p},\mathbf{k},\mathbf{r}} d\Phi_{\mathbf{p},\mathbf{k},\mathbf{r}} \sum_{s_{p,k,r}=\pm 1} [\mathrm{stat}]\, 2\pi\delta(\omega + s_p\omega_p + s_k\omega_k + s_r\omega_r) \\ f_c(\omega, s_p, s_k, s_r, \mathbf{p}, \mathbf{k}, \mathbf{r}) \tag{12}$$

where $c = 4, m$ and

$$d\Phi_{\mathbf{p},\mathbf{k},\mathbf{r}} = \frac{d^3\mathbf{p}}{(2\pi)^3 2\omega_p} \frac{d^3\mathbf{k}}{(2\pi)^3 2\omega_k} \frac{d^3\mathbf{r}}{(2\pi)^3 2\omega_r} (2\pi)^3 \delta(\mathbf{p} + \mathbf{k} + \mathbf{r}), \tag{13}$$

$$[\mathrm{stat}] = \frac{\cosh(\omega/2T)}{4\cosh(\omega_p/2T)\cosh(\omega_k/2T)\cosh(\omega_r/2T)}. \tag{14}$$

Spectral Densities

- The spectral densities may be written as

$$\rho_c(\omega) = 3 \int_{\mathbf{p},\mathbf{k},\mathbf{r}} d\Phi_{\mathbf{p},\mathbf{k},\mathbf{r}} \sum_{s_{p,k,r}=\pm 1} [\mathrm{stat}]\, 2\pi\delta(\omega + s_p\omega_p + s_k\omega_k + s_r\omega_r) \, f_c(\omega, s_p, s_k, s_r, \mathbf{p}, \mathbf{k}, \mathbf{r}) \tag{12}$$

where $c = 4, m$ and

$$d\Phi_{\mathbf{p},\mathbf{k},\mathbf{r}} = \frac{d^3\mathbf{p}}{(2\pi)^3 2\omega_p} \frac{d^3\mathbf{k}}{(2\pi)^3 2\omega_k} \frac{d^3\mathbf{r}}{(2\pi)^3 2\omega_r} (2\pi)^3 \delta(\mathbf{p} + \mathbf{k} + \mathbf{r}), \tag{13}$$

$$[\mathrm{stat}] = \frac{\cosh(\omega/2T)}{4\cosh(\omega_p/2T)\cosh(\omega_k/2T)\cosh(\omega_r/2T)}. \tag{14}$$

- In the large ω limit ($\omega \gg T \gg m$)

$$\rho_4(\omega) = \frac{5\omega^5}{2048\pi^3}\left(1 + \frac{112\pi}{3}\omega T^4 + \dots\right), \tag{15}$$

$$\rho_m(\omega) = \frac{7m\omega^4}{512\pi^3}\left(1 - \frac{4\pi^2 T^2}{\omega^2} + \dots\right). \tag{16}$$

On the Lattice

- In order to compute the lattice spectral densities we perform a two-loop summation over Brillouin zones.

On the Lattice

- In order to compute the lattice spectral densities we perform a two-loop summation over Brillouin zones.
- The maximum momenta (and hence energies) are given by the edges of the Brillouin zones. There are therefore lattice artifacts at large ω as these values of ω are excluded from the calculations of the spectral densities.

On the Lattice

- In order to compute the lattice spectral densities we perform a two-loop summation over Brillouin zones.
- The maximum momenta (and hence energies) are given by the edges of the Brillouin zones. There are therefore lattice artifacts at large ω as these values of ω are excluded from the calculations of the spectral densities.
- The structure of the spectral densities at large ω is familiar from similar studies of lattice meson spectral functions.

$\rho_4(\omega)$ scaled with $\omega^3 m^2$.

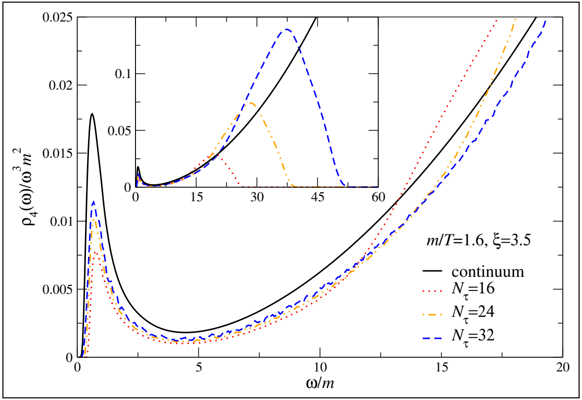

The finite temperature results demonstrate a thermal enhancement of $\rho_4(\omega)$ at $\omega \simeq m$. The values of $\rho_4(\omega)$ have been scaled with $\omega^3 m^2$ in order to better exhibit this enhancement.

$\rho_m(\omega)$ scaled with $\omega^3 m^2$.

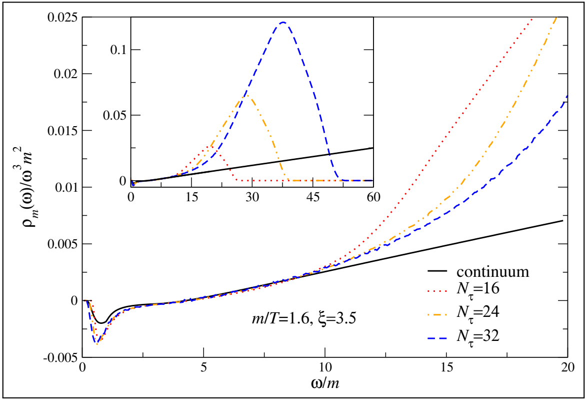

Again, a thermal enhancement at $\omega \simeq m$ at finite temperature is exhibited. Note: $\rho_m(\omega)$ is not positive definite.

Spectral Functions $\rho_{\pm}(\omega)$ Scaled with $\omega^3 m^2$ at $m/T = 2$.

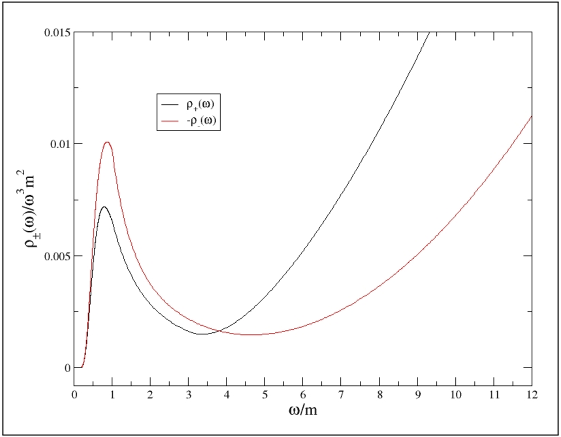

For large ω, $\rho_+(\omega) > -\rho_-(\omega)$, which is expected since $\rho_{\pm}(\omega) = 2\rho_m(\omega) \pm 2\rho_4(\omega)$.

Temperature dependence of $\rho_+(\omega)$

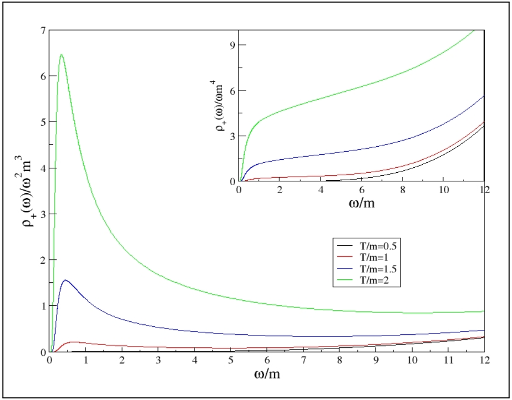

For decreasing temperature, the thermal enhancement is reduced, showing that the observed peaks are a finite temperature effect. The inset shows $\rho_+(\omega)$ with a different scaling, showing that these peaks are only visible apparent for certain choices of the renormalisation and do not correspond to any physical particle in the spectrum.

Chiral Symmetry

- In the massless case we expect that in the continuum $\rho_m(\omega) = 0$ and so $G_+(\tau) = -G_-(\tau) = G_+(1/T - \tau) = 2B_4(\tau)$.

Chiral Symmetry

- In the massless case we expect that in the continuum $\rho_m(\omega) = 0$ and so $G_+(\tau) = -G_-(\tau) = G_+(1/T - \tau) = 2B_4(\tau)$.
- However, on the lattice, the Wilson term breaks chiral symmetry for large momenta. This means that even at zero mass, $\rho_m(\omega) \neq 0$ and $G_+(\tau) \neq -G_-(\tau) \neq G_+(1/T - \tau)$.

Chiral Symmetry

- In the massless case we expect that in the continuum $\rho_m(\omega) = 0$ and so $G_+(\tau) = -G_-(\tau) = G_+(1/T - \tau) = 2B_4(\tau)$.
- However, on the lattice, the Wilson term breaks chiral symmetry for large momenta. This means that even at zero mass, $\rho_m(\omega) \neq 0$ and $G_+(\tau) \neq -G_-(\tau) \neq G_+(1/T - \tau)$.
- We can use the function $R(\tau)$ as a measure of the violation of chiral symmetry (parity doubling, see Chris Allton's talk), where

$$R(\tau) = \frac{G+(\tau) - G_+(1/T-\tau)}{G+(\tau) + G_+(1/T-\tau)} = \frac{G_m(\tau)}{G_4(\tau)}. \quad (17)$$

$R(\tau)$ may take the values $0 \leq R(\tau) \leq 1$, where $R(\tau) > 0$ when chiral symmetry is broken.

$G_+(\tau)$ and $-G_-(\tau)$ for $m = 0$.

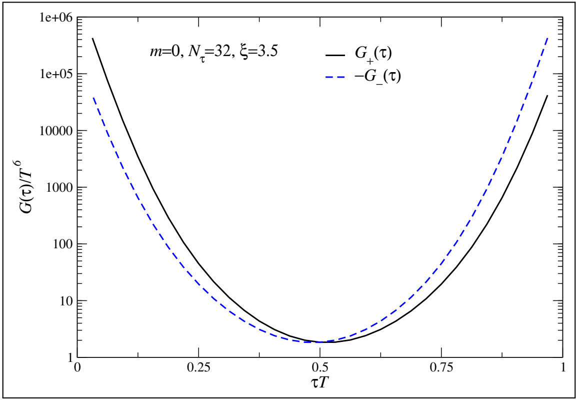

In the continuum, we expect that $G_+(\tau) = -G_-(\tau) = 2B_4(\tau)$. However, on the lattice, the Wilson term acts a mass term and hence $G_+(\tau) \neq -G_-(\tau)$.

$R(\tau)$ for varying N_τ, as we approach the continuum.

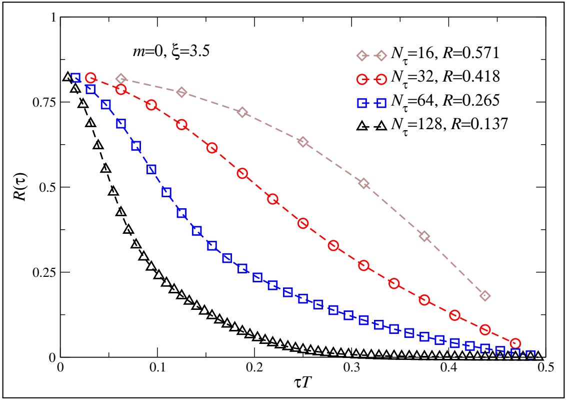

For finite lattice spacing $R(\tau) > 0$, hence chiral symmetry is broken at short distances. As we approach the continuum limit, $R(\tau)$ approaches zero.

A Comparison of the Lattice and Continuum Values for the Spectral Densities for $m = 0$

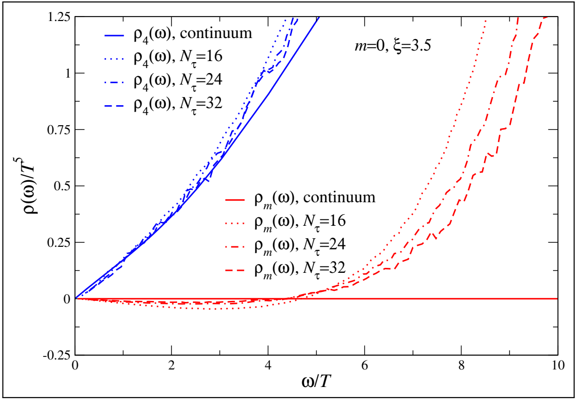

As the values of N_τ are increased, the values of $\rho(\omega)$ tend towards the continuum values, with $\rho_m(\omega)$ tending towards zero.

Conclusions

- The free field calculations of the baryon spectral densities involve a two loop calculation and so are more involved than for the case of mesons.

Conclusions

- The free field calculations of the baryon spectral densities involve a two loop calculation and so are more involved than for the case of mesons.
- Lattice artifacts at very large and very small values of ω arise from the sum over finite Brillouin zones, meaning that large momenta are inaccessible.

Conclusions

- The free field calculations of the baryon spectral densities involve a two loop calculation and so are more involved than for the case of mesons.
- Lattice artifacts at very large and very small values of ω arise from the sum over finite Brillouin zones, meaning that large momenta are inaccessible.
- Spectral densities at finite temperature exhibit thermal enhancement at $\omega \simeq m$.

Conclusions

- The free field calculations of the baryon spectral densities involve a two loop calculation and so are more involved than for the case of mesons.
- Lattice artifacts at very large and very small values of ω arise from the sum over finite Brillouin zones, meaning that large momenta are inaccessible.
- Spectral densities at finite temperature exhibit thermal enhancement at $\omega \simeq m$.
- At finite temperature, numerical results also exhibit chiral symmetry breaking due to the presence of the Wilson term. However, the results shown suggest that there is chiral symmetry restoration in the continuum limit, as expected.